Journal of the Meteorological Society of Japan, Vol. 89A, pp. 225–238, 2011.
DOI:10.2151/jmsj.2011-A14

Estimation and Verification of Daily Surface Shortwave Flux over China

Jianqing XU, Kooiti MASUDA

Research Institute for Global Change (RIGC), Japan Agency for Marine-Earth Science and Technology (JAMSTEC), Yokohama, Japan

Yasushi ISHIGOOKA, Tsuneo KUWAGATA

National Institute for Agro-Environmental Sciences (NIAES), Tsukuba, Japan

Shigenori HAGINOYA

Physical Meteorology Research Department, Meteorological Research Institute (MRI), Tsukuba, Japan

Tadahiro HAYASAKA

Graduate School of Science and Faculty of Science, Tohoku University, Sendai, Japan

and

Tetsuzo YASUNARI

Research Institute for Global Change (RIGC), Japan Agency for Marine-Earth Science and Technology (JAMSTEC), Yokohama, Japan
Hydrospheric Atmospheric Research Center (HyARC), Nagoya University, Nagoya, Japan

(Manuscript received 31 May 2010, in final form 19 October 2010)

Abstract

Downward shortwave flux at the surface over China was derived from sunshine duration data using parameters of Jordan sunshine recorders. The sunshine duration data were obtained as routine meteorological data and adjusted as necessary for the effects of topography, station surroundings, altitude, and atmospheric turbidity. Calculated flux was verified by in situ observations. Daily flux was calculated at more than 190 stations in China, Climatic maps (statistical period: 1971–2000) of surface solar radiation were produced and have been made public.

The sunshine duration-based shortwave flux was used to check satellite observation-based datasets. Two versions of satellite-based surface radiation budget datasets (SRB 2.0 and SRB 3.0) from NASA's Langley Research Center were investigated. Compared with the SRB 2.0 dataset, the SRB 3.0 dataset showed improved shortwave flux, especially over western China and the Tibetan Plateau.

1. Introduction

Global solar radiation is the energy resource of living things. Its variation and distribution are very important. Although meteorological data have become much more plentiful and accessible in recent years, daily data of downward shortwave flux at

Corresponding author: Jianqing Xu, Research Institute for Global Change (RIGC), Japan Agency for Marine-Earth Science and Technology (JAMSTEC), 3173-25 Showa-machi, Kanazawa-ku, Yokohama, 236-0001, Japan.
E-mail: jxu@jamstec.go.jp

the surface over wide areas are still lacking. To improve modeling, shortwave flux simulated by general circulation models (GCMs) and regional climate models should be checked using long-term observation-based data. In agriculture science, models including the photosynthetic process could also be improved by the use of daily shortwave flux data. Trenberth et al. (2009) and Kiehl and Trenberth (1997) summarized the Earth's annual global mean energy budget from satellite data. Satellite-based surface radiation budget (SRB) datasets are also available from NASA's Langley Research Center for the periods 1983–1995 (version 2.0) and 1983–2006 (version 3.0). To verify such satellite-based datasets, field observations of shortwave flux at the ground surface are needed, preferably covering long terms and even the period before satellite observations began.

In monsoon Asia, including parts of Japan and China, routine meteorological observations including daily measurements of sunshine duration have been recorded over long periods. For example, sunshine duration data have been recorded for more than 100 years at some stations in Japan, and many analyses have been conducted (Ichino et al. 2008; Inoue and Matsumoto 2003). In China, sunshine duration has been observed for more than 50 years. Past studies have used these data to analyze the trend of sunshine duration in China (Che et al. 2005; Kaiser and Qian 2002; Liang and Xia 2005b; Xu 2001; Xu et al. 2005b, 2009), but quantitative assessment of shortwave flux at the surface has not been previously reported.

To estimate surface shortwave flux in China, this study used observations of sunshine duration made using Jordan sunshine recorders (Fig. 1). This type of instrument is part of the standard observation equipment at surface meteorological stations in China and was also used at meteorological stations in Japan until the 1970s. The Jordan sunshine recorder determines the daily duration of bright sunshine. It consists of a copper cylinder with two small holes in its sides. One hole faces east, and the other faces west. The sunbeam penetrates the small holes, hitting light-sensitive paper inside the copper cylinder. The length of the band of changed color on the light-sensitive paper is a measure of sunshine duration. The paper is changed daily. This is a very simple observation method that needs no electricity and is easily maintained. The daily total direct solar radiation (integrated from sunrise to sunset) has a good statistical relationship with the observed daily duration of sunshine. Because most of the energy of daily mean downward shortwave flux at the surface (global solar radiation) is from direct solar radiation, shortwave flux at the surface can be estimated empirically from the daily duration of sunshine. This relationship was developed by means of both Jordan daily sunshine duration data and pyranometer instantaneous measurements of solar radiation (Kondo 1994). However, the Jordan recorder may not record times when the Sun is at low altitudes (about 5° in a city and 2° in a rural area). Yoshida (1970) analyzed this problem statistically and developed a revised method. Kondo and Xu (1996c) and Kondo et al. (1996) later revised the method for applications at high altitudes.

Fig. 1. Photograph of a Jordan sunshine recorder.

In this paper, we introduce a shortwave flux estimation method that adjusts for the effects of the topography, surroundings, and altitude of an observatory, as well as atmospheric turbidity. Satellite-based surface radiation budget (SRB)

datasets from NASA's Langley Research Center were also compared to estimations produced in this study. We discuss the method for calculating shortwave flux in section 2. Data adjustments are described in section 3, and results and comparisons with the satellite-based SRB data are presented in section 4. Section 5 contains a summary and conclusions.

2. Method of estimating downward shortwave radiation flux from sunshine duration

The method to estimate downward shortwave radiation flux at the surface from records of sunshine duration has been developed and described by Kondo (1994), Kondo and Xu (1996a, 1996b, 1996c), and Kondo et al. (1996). We summarize the method here.

The daily mean downward shortwave flux at the surface $S_M^{\downarrow}$ can be derived from sunshine duration N using parameters obtained from a Jordan sunshine recorder:

$$\frac{S_M^{\downarrow}}{S_0^{\downarrow}} = a_s + b_s \frac{N}{N_0}, \quad 0 < \frac{N}{N_0} \le 1, \tag{1}$$

and

$$\frac{S_M^{\downarrow}}{S_0^{\downarrow}} = c_s, \quad \frac{N}{N_0} = 0, \tag{2}$$

where N_0 is the possible duration of sunshine, and $S_0^{\downarrow}$ the daily mean of the downward shortwave flux at the top of the atmosphere. a_s, b_s, and c_s are empirical coefficients and depend on the type of the sunshine recorder, elevation, atmospheric turbidity, etc. These coefficients are decided empirically in Japan where the elevation is lower than 100 m asl (Kondo 1994). The elevation of observation stations in China varies from 0 m asl to more than 4,500 m asl. Thus, the effect of elevation was considered, following observation results over the Tibetan Plateau (Kondo et al. 1996). The coefficients a_s, b_s, and c_s depend on the surface pressure p_s as follows:

$$a_s = 0.179 + 0.32\left(1 - \frac{p_s}{1000}\right), \tag{3}$$

$$b_s = 0.55, \tag{4}$$

$$c_s = 0.114 + 0.32\left(1 - \frac{p_s}{1000}\right). \tag{5}$$

Here, N_0 is determined by the latitude. N_0 and $S_0^{\downarrow}$ are given by

$$N_0 = 2\zeta \frac{24}{2\pi} = \frac{2\zeta}{0.2618}, \tag{6}$$

where

$$\zeta = \cos^{-1}\left(\frac{\sin\alpha - \sin\phi \sin\delta}{\cos\phi \cos\delta}\right), \tag{7}$$

and

$$S_0^{\downarrow} = \frac{S_{00}}{\pi} d(\zeta \sin\phi \sin\delta + \cos\phi \cos\delta \sin\zeta), \tag{8}$$

where

$$d = 1.00011 + 0.034221 \cos\eta + 0.00128 \sin\eta + 0.000719 \cos 2\eta + 0.000077 \sin 2\eta, \tag{9}$$

$$\delta = \sin^{-1}(0.398 \times \sin(4.871 + \eta + 0.033 \sin\eta)), \tag{10}$$

and

$$\eta = \frac{2\pi}{365} Day. \tag{11}$$

In the above equations, S_{00} is the solar constant, ζ is the half-day angle, α (radians) is the solar altitude, ϕ is the latitude, δ is the solar declination, and Day is the number of days from 1 January to the observation day.

The daily mean of the downward shortwave flux at the surface under clear skies ($S_{\mathrm{Mf}}^{\downarrow}$) is (Kondo 1994)

$$\frac{S_{\mathrm{Mf}}^{\downarrow}}{S_0^{\downarrow}} = (C_1 + 0.7 \times 10^{-k_3 m_{\mathrm{noon}} F_1})(1 - i_3)(1 + j_1), \tag{12}$$

where

$$i_3 = 0.014(k_3 m_{\mathrm{noon}} + 7 + 2 \log_{10} w) \log_{10} w, \tag{13}$$

$$m_{\mathrm{noon}} = (p_s/p_0) \sec(\phi - \delta), \quad \phi - \delta < \pi/2, \tag{14}$$

$$m_{\mathrm{noon}} = \infty, \quad \phi - \delta \ge \pi/2, \tag{15}$$

$$k_3 = 1.042 - 0.06 \log_{10}(\beta_{\mathrm{DUST}} + 0.02) - 0.1(\sec(\phi - \delta) - 0.091)^{1/2}, \tag{16}$$

$$C_1 = 0.21 - 0.2\beta_{\mathrm{DUST}}, \quad \beta_{\mathrm{DUST}} < 0.3, \tag{17}$$

$$C_1 = 0.15, \quad \beta_{\mathrm{DUST}} \ge 0.3, \tag{18}$$

$$F_1 = 0.056 + 0.16(\beta_{\mathrm{DUST}})^{1/2}, \tag{19}$$

and

$$j_1 = [0.066 + 0.34(\beta_{\mathrm{DUST}})^{1/2}](ref - 0.15). \tag{20}$$

where p_0 (= 1,013 hPa) is the standard atmospheric pressure, *ref* the ground surface albedo, β_{DUST} is the atmospheric turbidity defined by Robinson (1966), and w the precipitable water (cm) estimated as

$$\log_{10} w \approx \log_{10} w^* + 0.10. \tag{21}$$

Here, w^* is the effective precipitable water,

$$w^* = \frac{1}{g}\int_0^{p_s} q\frac{p}{p_0}dp. \tag{22}$$

Where q is the specific humidity of air. Because we had no observed aerological q data, an empirical method (Kondo and Xu 1996c) was used here. The method was developed from observed aerological data of China. Dew point T_{DEW} can be calculated from the surface air vapor pressure e,

$$T_{DEW} = \frac{237.3 \times \log_{10}(e/6.1078)}{7.5 - \log_{10}(e/6.1078)}, \tag{23}$$

and,

$$\log_{10} w^* = 0.027T_{DEW} - 0.15 - x_0, \quad T_{DEW} < -5^\circ\mathrm{C}, \tag{24}$$

$$\log_{10} w^* = 0.031T_{DEW} - 0.13 - x_0, \quad -5^\circ\mathrm{C} \le T_{DEW} < 23^\circ\mathrm{C}, \tag{25}$$

$$\log_{10} w^* = 0.015T_{DEW} + 0.238 - x_0, \quad 23^\circ\mathrm{C} \le T_{DEW} < 30^\circ\mathrm{C}, \tag{26}$$

Here,

$$x_0 = 1 - \left(\frac{p_s}{1013.2}\right)^{0.5}. \tag{27}$$

If the change in precipitable water with elevation is considered (in this paper, where the elevation is higher than 100 m asl), a_s can be expressed as,

$$a_s = (0.21 + 0.7 \times 10^{-0.056Y})(1 - i_3) - b_s, \tag{28}$$

where

$$Y = 1.45\left(\frac{p_s}{1013}\sec(\phi - \delta)\right), \tag{29}$$

where i_3 is shown in Eq. 13.

3. Data, data adjustments, and verifications

3.1 Data

1) Satellite-based data

Among several global satellite-based data products of radiation at the surface, we use the NASA/GEWEX Surface Radiation Budget (SRB) data set produced by the SRB team led by Paul Stackhouse of NASA's Langley Research Center, Hampton, Virginia. Information about the dataset is available at http://eosweb.larc.nasa.gov/PRODOCS/srb/table_srb.html.

The time resolution is 3 hours, and the spatial resolution is 1 degree latitude/longitude. The SRB Shortwave (SW) Release 2.0 covers July 1983 to October 1995, and Release 3.0 covers July 1983 to June 2006. Both versions are based on cloud information compiled as the pixel-level (DX) dataset of the International Satellite Cloud Climatology Project (ISCCP, Rossow and Schiffer 1999) and the algorithm developed by Pinker and Laszlo (1992). However, many practical improvements were made between the two versions.

From SRB 2.0 to 3.0, several steps were entailed in updating the versions, for example, fixing the deficits in the polar night, using the cloud amount in the calculation, reforming the solar zenith angle, etc. In particular, comparison with experimental ground-based observations revealed substantial underestimation over the Tibetan Plateau in SRB SW Release 2.5 (Yang et al. 2006); the lessons learned have been incorporated in the revision of the algorithm. A major difference between SRB 2.5 and SRB 2.81 is that the lookup tables in the radiative transfer code of SRB 2.5 do not account for levation and its effect on Rayleigh scattering, whereas this effect was included in SRB 2.81 (Yang et al. 2008).

In the present study, monthly climatological values of both SRB 2.0 and 3.0 were calculated using all available months. Then, values at the grid boxes nearest to observation stations were extracted and compared with those estimated at the stations in the present study.

2) Routine meteorological data

The routine meteorological data were provided by the China Meteorological Data Sharing Service System (http://cdc.cma.gov.cn/) of the China Meteorological Administration for a period from the 1950s to 2006. The data used in the present study include the following:

- sunshine duration N (hour)
- daily mean vapor pressure e (hPa)
- surface pressure p_s (hPa)

Atmospheric turbidity β_{DUST}, as defined by Robinson (1966), was assumed in the calculation of $S^{\downarrow}_{\mathrm{Mf}}$.

Fig. 2. Picture of the Deqen observatory (28°29′N, 98°55′, 3,320 m asl), which is located in a valley surrounded by high mountains. Raw sunshine duration data for Deqen were revised.

3.2 Data adjustments

Some observatories are located in valleys (Fig. 2), such as Deqen (31°25′N, 95°36′E, 3,875 m asl) observatory, which is located in a valley surrounded by mountains, while others are situated in urban canyons. When discussing the trend of sunshine duration, problems associated with such locations can be ignored. However, if we want to quantitatively assess the distribution of shortwave flux at the surface, the raw data should be revised. Thus, we considered the effects of topography, and surroundings to adjust the data of sunshine duration.

If a meteorological station is located in a valley or surrounded by high buildings, the observed sunshine duration N_{Obs} may be less than its true value. Under clear sky condition, N_{Obs}/N_0 should be near 1.0, but the Jordan sunshine recorder records only the duration of bright sunshine. If the solar altitude is too low (about 5° in the city and 2° in rural areas), the sunlight will be too weak to be recorded by the light-sensitive paper. Generally, the maximum of the ratio N_{Obs}/N_0 is 0.92–1.00. We modified the observed sunshine duration N_{Obs} to derive the representative value N, which was then applied to Eq. 1. For such a case, we assumed that $N = N_{\mathrm{Obs}}$. The reference of the minimum direct solar radiation is defined as 120 W m^{-2} because the shadow of objects is hard to recognize when direct solar radiation is less than 120 W m^{-2}. However, if the ratio of N_{Obs}/N_0 under clear-sky condition is always shows a low value, for example, less than 0.9, the station may be in a valley or surrounded by high buildings and the observed raw data N_{Obs} should be adjusted.

The theoretical possible duration of sunshine N_0 can be calculated from Eq. 6 when the latitude is known. In Eq. 7, α is the solar altitude and repre-

sents the time of sunset in a valley. The half-day angle ζ can be obtained, and the possible duration of sunshine N_0' in a valley can be calculated from Eq. 6. The ratio N_{Obs}/N_0' is used to revise the dataset through the following empirical formulas (Kondo et al. 1996):

$$\frac{N}{N_0} = \frac{N_{\mathrm{Obs}}}{N_0'} - \Delta, \tag{30}$$

$$\Delta = f\{1 - \exp[-0.085(\varepsilon - 2)]\}, \tag{31}$$

$$f = \frac{N_{\mathrm{Obs}}}{N_0'} \times \frac{0.23}{1 + \left[\tan\left(\frac{N_{\mathrm{Obs}}}{N_0'}\right) - 0.2\right]^{10}}. \tag{32}$$

where ε is the emissivity of ground-surface. Figure 3 shows examples of observed raw sunshine duration data. The solid lines show seasonal changes at different solar altitudes $(2^\circ, 4^\circ, \ldots, 20^\circ)$. The upper panel is for Jiuquan (39°46′N, 98°29′E, 1,477 m asl), and the lower panel is for Baingoin (31°22′N, 90°01′E, 4,700 m asl). At Jiuquan, N_{Obs}/N_0 exceeds 0.9 and is plotted around 2°–4° of the solar altitude. The meteorological observatory at Jiuquan is in an open area without nearby mountains or buildings, and thus $N = N_{\mathrm{Obs}}$ at this station. In contrast, at Baingoin, N_{Obs}/N_0 is sometimes less than 0.9 and is plotted between 4° *and* 7°. Sunlight is blocked when the solar altitude is less than about 5°. Baingoin may be in a valley on the Tibetan Plateau, where $N \neq N_{\mathrm{Obs}}$.

Figure 4 shows seasonal changes in the ratios of sunshine duration. The top panel presents observed raw data, the middle panel shows adjusted data, and the bottom panel gives precipitation at Baingoin in 1998. The revised sunshine duration is reasonable. This kind of data checking was conducted for all of the stations.

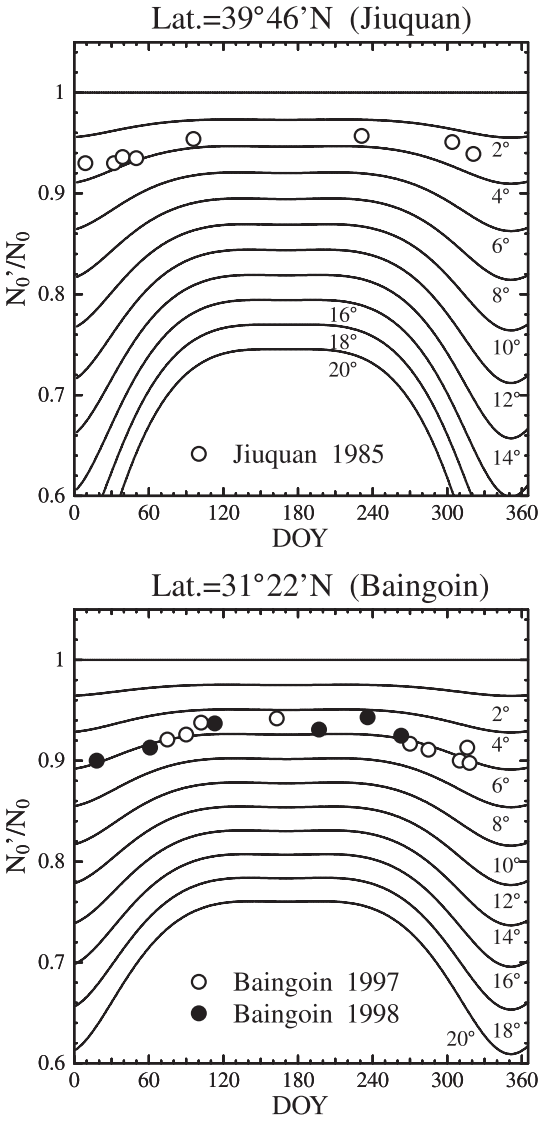

Fig. 3. Checking of sunshine duration data. Solid lines show the seasonal changes at different solar altitudes $(2^\circ, 4^\circ, \ldots, 20^\circ)$. The upper panel is for Jiuquan (39°46′N, 98°29′E, 1,477 m asl), and the lower panel is for Baingoin (31°22′N, 90°01′E, 4,700 m asl). The circles mark N_{Obs}/N_0 on fine days.

3.3 *Verifications of the downward shortwave flux at the surface*

1) *Shortwave flux at the surface under clear-sky conditions* $S^{\downarrow}_{\mathrm{Mf}}$

The calculation of daily mean downward shortwave flux at the surface under clear-sky conditions $S^{\downarrow}_{\mathrm{Mf}}$ used atmospheric turbidity β_{DUST} as defined by Robinson (1966). In fact, atmospheric turbidity has its seasonal change. In this study, we assumed it as a constant. Assuming that the atmospheric turbidity β_{DUST} as a constant changes between 0 *and* 0.1 (for example, $\beta_{\mathrm{DUST}} = 0.01, 0.02, \ldots, 0.10$), $S^{\downarrow}_{\mathrm{Mf}}$ can be obtained for different β_{DUST} when the latitude is known. If the calculated daily mean of shortwave flux $S^{\downarrow}_{M}$ (input data is N only) under clear sky conditions (when $N/N_0 \geq 0.9$) is adjusted with the most suitable $S^{\downarrow}_{\mathrm{Mf}}$, then β_{DUST} can be determined.

Figure 5 shows the seasonal changes of calculated shortwave flux at Jiuquan in 1985. The solid line is the daily mean shortwave flux $S^{\downarrow}_{M}$ estimated from sunshine duration N. The dotted line is the

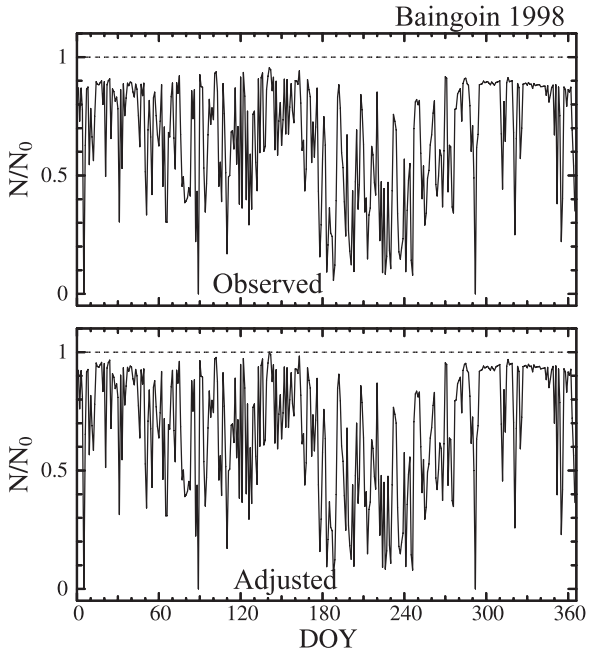

Fig. 4. Seasonal changes in the ratios of sunshine duration N/N_0. The top panel presents raw observed data, and the bottom panel shows revised data Baingoin in 1998.

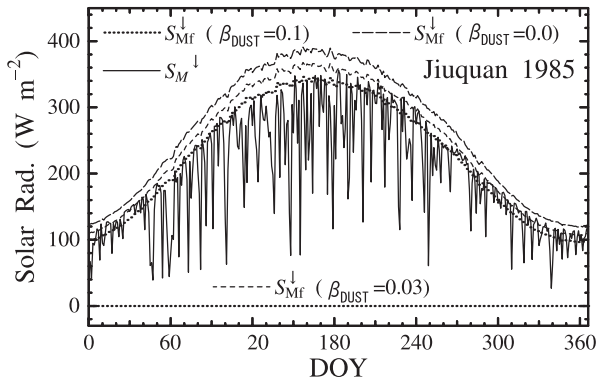

Fig. 5. Seasonal changes in calculated downward shortwave fluxes at Jiuquan in 1985. The solid line represents the daily shortwave flux $S_M^{\downarrow}$ as estimated from sunshine duration. The dotted line represents the daily downward shortwave fluxes under clear-sky conditions $S_{\mathrm{Mf}}^{\downarrow}$ when $\beta_{\mathrm{DUST}} = 0.1$. The broken line is $S_{\mathrm{Mf}}^{\downarrow}$ when $\beta_{\mathrm{DUST}} = 0.03$, and the dashed line is $S_{\mathrm{Mf}}^{\downarrow}$ when $\beta_{\mathrm{DUST}} = 0.0$.

daily mean shortwave flux under clear-sky conditions $S_{\mathrm{Mf}}^{\downarrow}$ when $\beta_{\mathrm{DUST}} = 0.1$. The broken line is $S_{\mathrm{Mf}}^{\downarrow}$ when $\beta_{\mathrm{DUST}} = 0.03$. The dashed line is $S_{\mathrm{Mf}}^{\downarrow}$ when $\beta_{\mathrm{DUST}} = 0.0$. When $\beta_{\mathrm{DUST}} = 0.03$, $S_{\mathrm{Mf}}^{\downarrow}$ adjusts $S_M^{\downarrow}$ well, and β_{DUST} is assumed to be 0.03 in Jiuquan. In the winter time, β_{DUST} may be less than 0.03, but the solar energy in the winter time is less than that in the summer time.

Atmospheric turbidity β_{DUST} was estimated for every meteorological station for determination of a suitable $S_{\mathrm{Mf}}^{\downarrow}$. β_{DUST} ranges between 0.01 and 0.10 in present study. This $S_{\mathrm{Mf}}^{\downarrow}$ and calculated $S_M^{\downarrow}$ are independent under clear-sky conditions (when $N/N_0 \geq 0.9$). The calculated $S_M^{\downarrow}$ was checked by $S_{\mathrm{Mf}}^{\downarrow}$. If $S_M^{\downarrow}$ (observed N) is over its theoretical value ($S_{\mathrm{Mf}}^{\downarrow}$), it is replaced by the climatic value (30-year mean value in 1971–2000) for the same day.

2) Verification of the downward shortwave flux at the surface from observed data

The calculated shortwave flux has been compared with observations at Beijing (39°48′N, 116°28′E, 54 m asl) and Lhasa (29°40′N, 91°08′E, 3650 m asl). The observed $S_M^{\downarrow}$ of Beijing was downloaded from the China Meteorological Data Sharing Service System (http://cdc.cma.gov.cn/) of the China Meteorological Administration. Lhasa is located at a high altitude, 3650 m, and no observed shortwave flux data were available from routine meteorological station records. Pyranometers (Ishikawa Industry, A2-S-180) were installed at Lhasa, where observations were conducted in cooperation with specialists from Ishikawa Industry. The pyranometers were exchanged every year and recalibrated in the factory. Sunshine duration N was observed at the Lhasa meteorological station. These observations were part of the automated weather station (AWS) observations of the Global Energy and Water Cycle Experiment (GEWEX) Asian Monsoon Experiment (GAME)-Tibet project. Data from these pyranometers have been utilized by Xu and Haginoya (2001), and Xu et al. 2005a.

Figure 6 shows the shortwave flux as observed and calculated (from sunshine duration N) at Lhasa in 1996 (Fig. 6a,b) and Beijing in 1999 (Fig. 6c,d). The same parameters were used to estimate shortwave flux at both stations. β_{DUST} was 0.01 at both stations. The annual mean shortwave flux was 240 W m^{-2} at Lhasa and 160 W m^{-2} at Beijing. From the regression analysis, the observed value was larger than the calculated value when the shortwave flux was small, and the situation

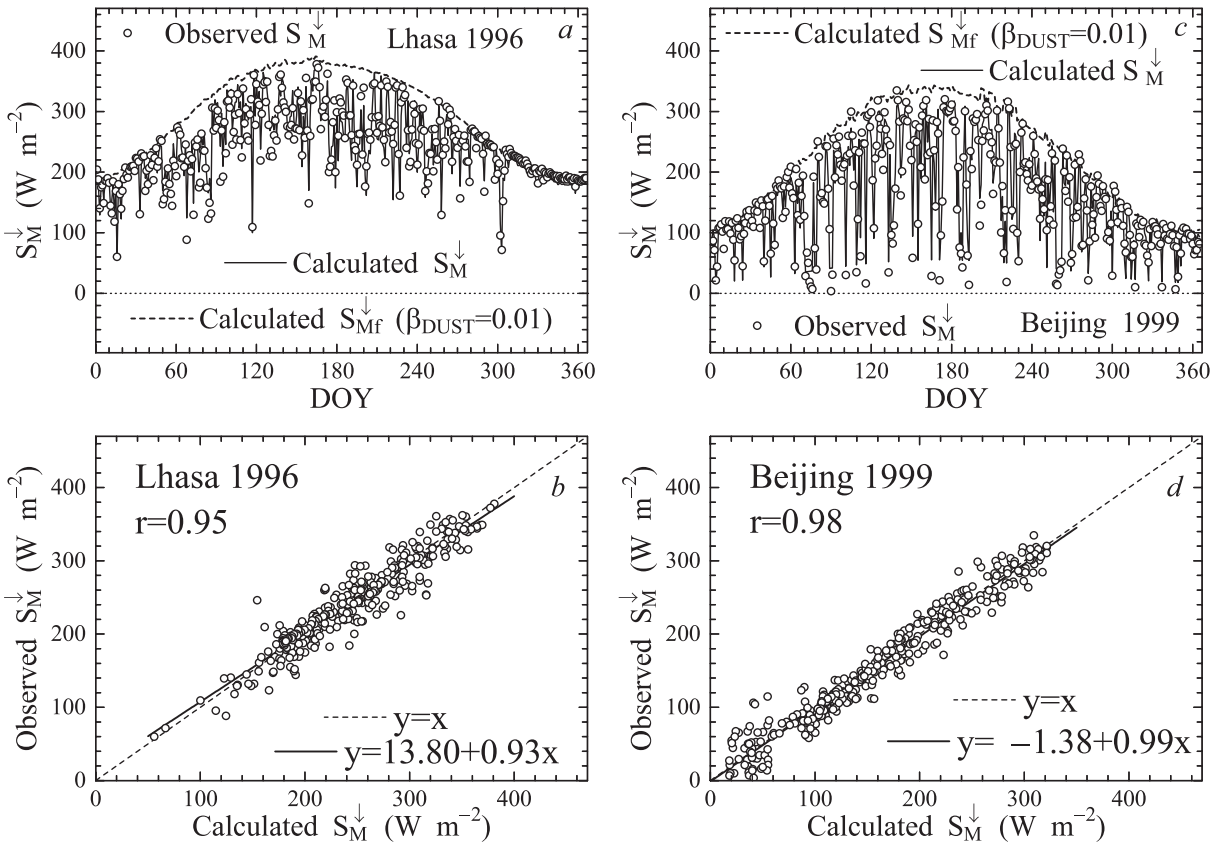

Fig. 6. Calculated and observed daily mean shortwave flux at the surface in Lhasa (1996) and Beijing (1999). *a*) seasonal variation in shortwave flux at the surface by pyranometer observations and calculations from sunshine duration N for Lhasa in 1996. The solid line is the calculated $S_M^{\downarrow}$ from N. The dotted line is $S_{\mathrm{Mf}}^{\downarrow}$ under clear-sky conditions with Robinson's atmospheric turbidity β_{dust} of 0.01. Circles represent $S_M^{\downarrow}$ observed by pyranometer; *b*) regression analysis of the observed and calculated $S_M^{\downarrow}$; *c*) the same as *a*) except for Beijing 1999; *d*) the same as *b*) except for Beijing 1999.

was reversed when the shortwave flux became large. The maximum differences between the observed and calculated values were about 10 W m^{-2} at Lhasa and 3–5 W m^{-2} in Beijing. The maximum estimation errors were less than 10% at both stations. These results indicate that the calculated values well matched the observations. The coefficient of correlation was 0.98 at Beijing and 0.95 at Lhasa. The range of daily mean shortwave flux was about 80 W m^{-2}–380 W m^{-2} at Lhasa and about 20 W m^{-2}–320 W m^{-2} at Beijing.

So far, all of the data have been checked, and the calculation method has been verified. Calculation results (see the solid lines in Fig. 6a,c as examples) for the period from the 1950s to 2006 were obtained daily for 194 stations in China, including the Tibetan Plateau. This data set was derived from sunshine duration data, with the time resolution set as daily because the daily data of downward shortwave flux at the surface over wide areas are needed for recent years.

4. Estimation results

Of course, the climatic distribution of the solar radiation can be drawn directly from the observed sunshine duration time, and its unit will be hours. This kind of dataset is inconvenient for checking the shortwave flux results from the GCMs or for use as the input data for agricultural models. In this study, we provide the absolute value of the solar radiation flux in W m^{-2} units.

Here, we only show the climatological normal values of downward shortwave flux at the surface during 1971 to 2000.

4.1 *Climatic distribution of shortwave flux at the surface in China*

Figure 7 shows the distribution of shortwave flux at the surface annually, in January, and in July. The annual and monthly data are made public at the daily shortwave flux during 1971–2000 (http://www.jamstec.go.jp/drc/maps/d/kadai/mon/mon_ea.html). Annual shortwave flux is small over the Sichuan Basin (120–140 W m^{-2}) and large over the Tibetan Plateau (240–260 W m^{-2}) because Sichuan Basin is always covered by cloud, and the sunshine duration is shorter than other places at the same latitude. From the Tibet Plateau to northwest China, the climate is arid or semi-arid and is marked by many clear days. The sunshine duration is longer in these areas.

In winter (January), shortwave flux is less than 80 W m^{-2} in the Sichuan Basin and about 150 W m^{-2} in southeastern Tibetan Plateau. The contrast in the distribution of shortwave flux between the Sichuan Basin and the Plateau becomes more obvious in the winter time.

In summer (July), from Sichuan Basin through southeast China to the southern part of northeast China, the shortwave flux is relatively small because the Asian monsoon brings cloudy and rainy days, and the sunshine duration is short in this season.

4.2 *Comparison with solar radiation flux from Langley SRB datasets*

We compared both the Langley SRB2.0 and SRB3.0 datasets to our calculated shortwave flux at the surface. Figure 8a presents the distribution of data from the observatories. In the case of the Langley SRB2.0 dataset, data performances are poor in both the Tibetan and western China areas (Fig. 8b,c). However, the newer Langley SRB3.0 dataset agrees with our dataset well in winter (January, Fig. 8d) and shows improved performance compared with SRB2.0 in summer (July, Fig. 8e). The dataset produced in this study provides a relatively standard dataset (daily) for checking other datasets. SRB3.0 products differ substantially from SRB2.0 owing to numerous improvements of the algorithms and input data sets (http://eosweb.larc.nasa.gov/PRODOCS/srb/table_srb.html).

4.3 *Comparison of interannual variations between calculated shortwave flux and SRBs*

SRB3.0 products have been improved from SRB2.0, and its value are more closer to the calculated shortwave flux in the present study, especially in the areas of Tibet and western China.

Beijing is located in the eastern region, and Lhasa in the Tibetan region. The values from both SRB 2.0 and 3.0 were extracted at the grid boxes nearest to observation stations. Figure 9 shows the monthly mean value of shortwave flux ($S_M^{\downarrow}$: solid line) for Beijing (lower panel) and Lhasa (upper panel) from 1984 to 1994 (the period of SRB 2.0). The variation of satellite based $S_M^{\downarrow}$ (SRB2.0 and SRB 3.0) matches that of calculated $S_M^{\downarrow}$ well in every month in Beijing, but values of calculated $S_M^{\downarrow}$ are smaller than those of SRB $S_M^{\downarrow}$. Averaged value of calculated $S_M^{\downarrow}$ is 164 W m^{-2}, SRB 2.0 $S_M^{\downarrow}$ is 180 W m^{-2}, and SRB 3.0 $S_M^{\downarrow}$ is 183 W m^{-2} during 1984–1994.

In the case of Lhasa (upper panel in Fig. 9), the averaged value of calculated $S_M^{\downarrow}$ is 242 W m^{-2}, SRB 2.0 $S_M^{\downarrow}$ 202 W m^{-2}, and SRB 3.0 $S_M^{\downarrow}$ 231 W m^{-2} during 1984–1994. The SRB 2.0 value was too small, and the SRB 3.0 value was better than SRB 2.0 if the calculated $S_M^{\downarrow}$ was considered as the standard value. As mentioned in Section 3.a.1, the improvement from SRB2.0 to SRB 3.0 was mainly observed considering the influence of the Tibetan Plateau (Yang et al. 2006, 2008). For plain-field areas such as Beijing, no improvement was apparent.

5. Summary and conclusion

A method to estimate downward shortwave flux has been developed and applied over a wide area of China. Shortwave flux was estimated from sunshine duration data using parameters measured by Jordan sunshine recorders. The raw data of sunshine duration were revised, considering the effects of the topography, surroundings, and altitudes of observation stations. The influence of atmospheric turbidity was also considered. Calculated values were verified by in situ observations.

The results show the climatic distribution of shortwave flux. The estimated daily shortwave flux has many research uses, such as for verification of other databases. Two Langley SRB datasets were checked using the shortwave flux obtained in this study. The SRB3.0 dataset was improved compared with the SRB2.0 dataset for a high altitude area (Tibet) and an arid area (West China). Our dataset can also be compared with the output from GCMs and regional climatic models. In agricultural research, models incorporating the photosynthetic process of vegetation can also be improved by using these daily shortwave flux data.

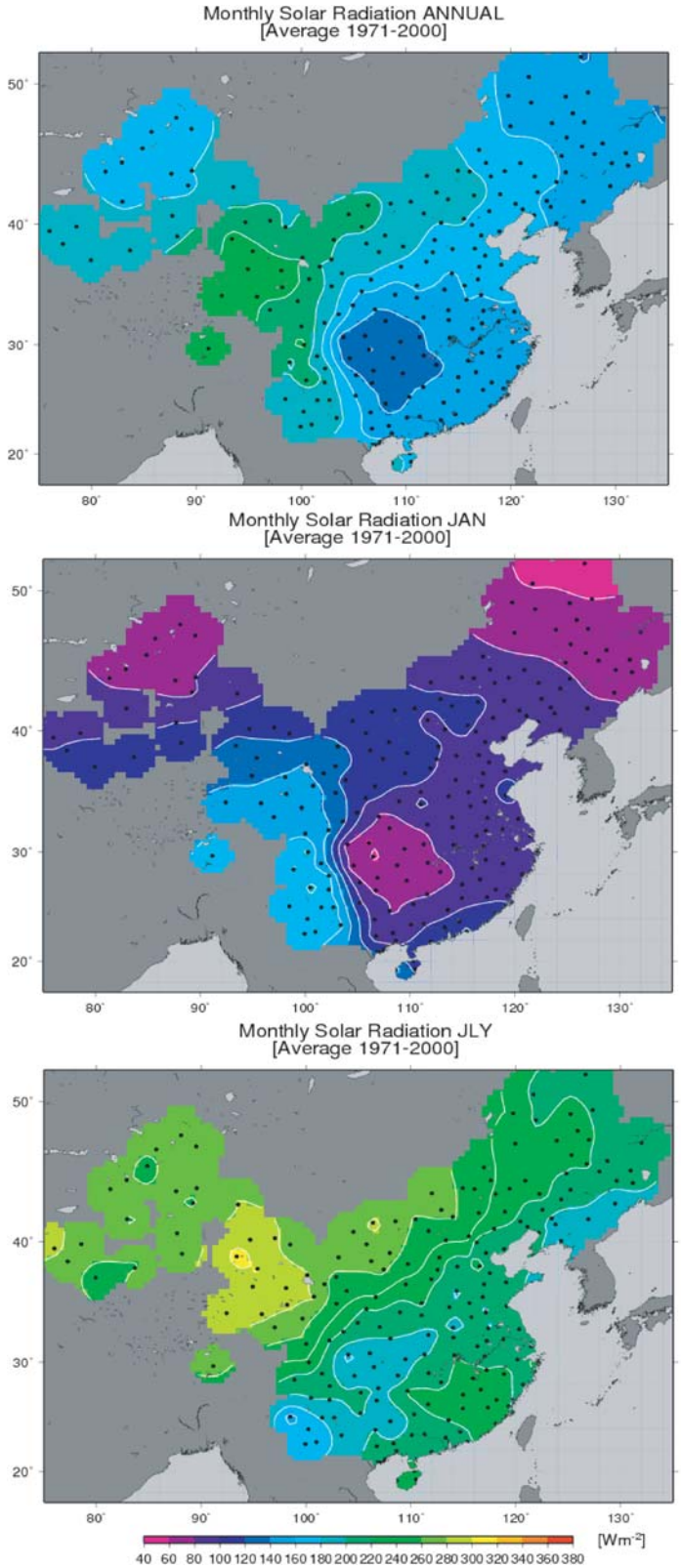

Fig. 7. Distributions of climatological shortwave flux at the surface annually (upper panel), in January (middle panel), and in July (bottom panel). Black spots show the distribution of the stations.

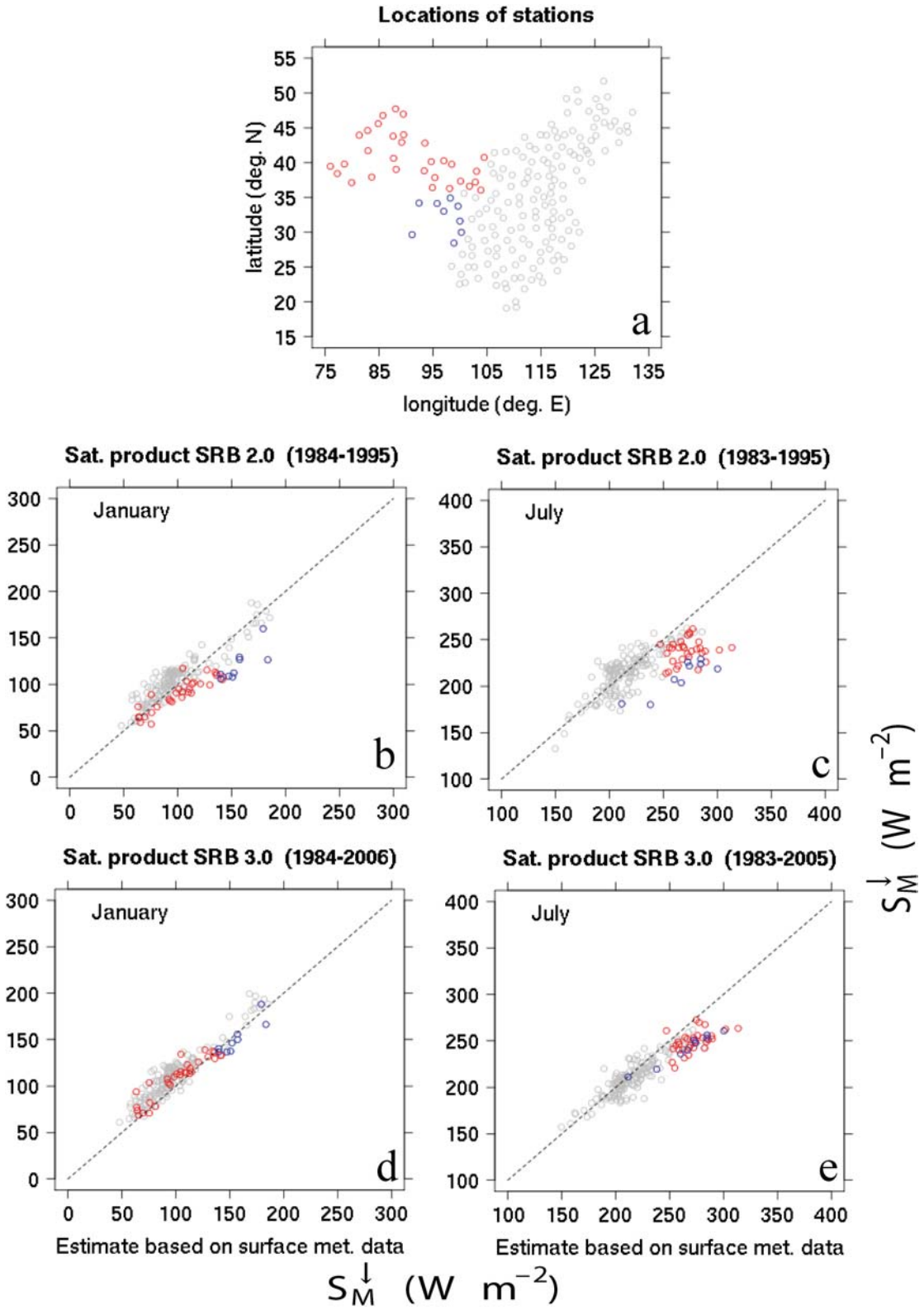

Fig. 8. a) Distribution of the $S_M^{\downarrow}$ data at the observatories. Blue circles represent the Tibetan area (high altitude), and red circles denote western China (arid). Relationships between b) Langley SRB2.0 data and the present data in January, c) Langley SRB3.0 data and the present data in January, d) Langley SRB2.0 data and the present data in July, and e) Langley SRB3.0 data and the present data in July.

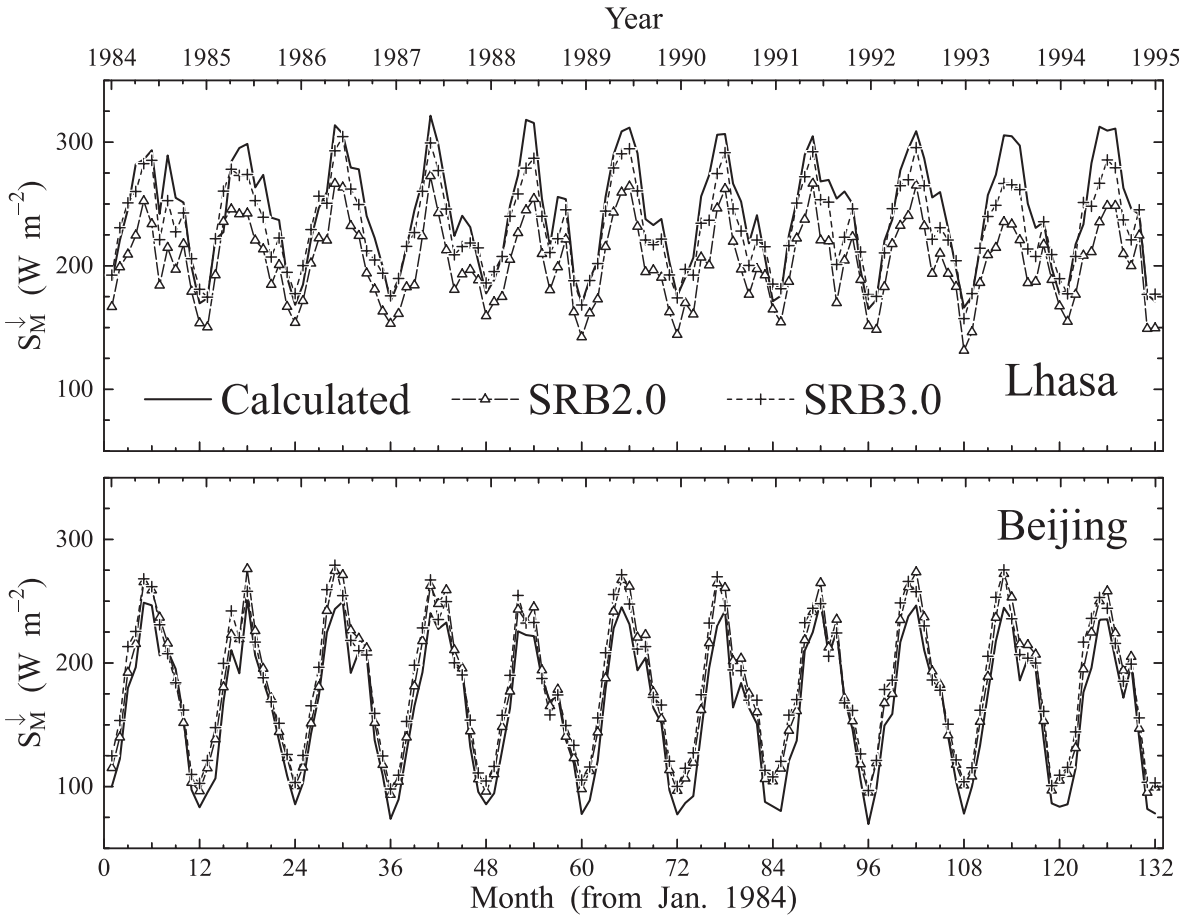

Fig. 9. Interannual variations in the downward shortwave expressed by monthly mean values at Beijing (lower panel) and Lhasa (upper panel) during 1984–1994. The solid lines represent the calculated monthly mean value of downward shortwave flux $S_M^{\downarrow}$, the triangles with dashed lines show the downward shortwave flux from Langley SRB2.0, and the plus signs with broken line are from Langley SRB3.0 data. Numbers on the upper x-axis show years and are placed at the beginning of individual years. Numbers on the lower x-axis represent the sequential number of months, where 1 corresponds to January 1984.

Acknowledgments

The authors thank Dr. Kazuyo Fukuda of the Japan Agency for Marine Earth Science and Technology (JAMSTEC) for making the figures for the internet publication of this dataset. We also thank the China Meteorological Data Sharing Service System (http://cdc.cma.gov.cn/) of the China Meteorological Administration for providing the data. Thanks are also extended to NASA's Langley Research Center Atmospheric Sciences Data Center NASA/GEWEX SRB Project for proving the SRB datasets. We thank the referee for providing constructive comments and help in improving the contents of this paper. This study was supported by data Integration and Analysis System (DIAS). The study was also supported by JSPS and China NSFC under the Japan–China Scientific Cooperation Program 'A study of water and heat circulation in the Nam Co Basin using remote sensing and in situ observation data,' Grants-in-Aid for Scientific Research of JSPS (No. 22310016), and 'Impact of Asian Megacity Development on Local to Global Climate Change' under the Strategic Japanese–Chinese Cooperative Program on Climate Change between JST and MOST.

Appendix

Notation

a_s	one of the coefficients of Jordan sunshine recorder
b_s	one of the coefficients of Jordan sunshine recorder
c_s	one of the coefficients of Jordan sunshine recorder
e (hPa)	observed daily mean vapor pressure
N (hour)	observed sunshine duration
N_{Obs} (hour)	observed sunshine duration (raw data)
N_0 (hour)	duration of possible sunshine
p_s (hPa)	observed surface pressure
q	specific humidity of air
ref	albedo of ground surface
$S_M^{\downarrow}$ (Wm^{-2})	daily mean downward surface shortwave radiation flux
$S_{\mathrm{Mf}}^{\downarrow}$ (Wm^{-2})	$S_M^{\downarrow}$ under clear sky
$S_0^{\downarrow}$ (Wm^{-2})	downward surface shortwave radiation flux at the top of the atmosphere
S_{00} (Wm^{-2})	solar constant (1365 Wm^{-2})
T_{DEW}(°C)	dew point
w (cm)	precipitable water
α (rad)	sun's altitude
β_{DUST}	Robinson's atmospheric turbidity
ε	emissivity of ground-surface
δ (rad)	solar declination
ζ (rad)	half-day angle
ϕ (rad)	latitude

References

Che, H. Z., G. Y. Shi, X. Y. Zhang, R. Arimoto, J. Q. Zhao, L. Xu, B. Wang, and Z. H. Chen, 2005: Analysis of 40 years of solar radiation data from China, 1961–2000, *Geophys Res Lett*, **32**, doi:10.1029/2004GL022322.

Ichino, M., J. Xu, and K. Masuda, 2008: Estimation of shortwave flux at the surface and its variability in the last 100 years at Tokyo. *Proceeding of Meteorol. Soc. Japan.*, **95**, 395 (in Japanese).

Inoue, T., and J. Matsumoto, 2003: Seasonal and secular variations of sunshine duration and natural seasons in Japan. *Int. J. Climatol.*, **23**, 1219–1234.

Kaiser, D. P., and Y. Qian, 2002: Decreasing trends in sunshine duration over China for 1954–1998: Indication of increased haze pollution? *Geophys. Res. Lett.*, **29**, doi:10.1029/2002GL016057.

Kiehl, J. T., and K. E. Trenberth, 1997: Earthfs annual global mean energy budget *Bull. Amer. Meteor. Soc.*, **78**, 197–208.

Kondo, J., 1994: *Meteorology of the Water Environment—Water and Heat Balance of the Earth's Surface*. Asakura Shoten Press, Japan, 348 pp (in Japanese).

Kondo, J., and J. Xu, 1996a: An estimation of heat balance for arid and semi-arid regions in China (1): climatological conditions, soil parameters and calculation method. *J. Japanese Soc. Hydro. and Water Resour.*, **9**, 162–174 (in Japanese with English abstract).

Kondo, J., and J. Xu, 1996b: An estimation of heat balance for arid and semi-arid regions in China (2): results. *J. Japanese Soc. Hydro. and Water Resour.*, **9**, 175–187 (in Japanese with English abstract).

Kondo, J., and J. Xu, 1996c: Empirical formula for estimating the precipitable water from the dew-point temperature at the ground level. *J. Japanese Soc. Hydro. and Water Resour.*, **9**, 463–467 (in Japanese with English abstract).

Kondo, J., J. Xu, and S. Haginoya, 1996: Empirical formula for estimating the solar radiation at an upland from the sunshine duration data. *J. Japanese Soc. Hydro. and Water Resour.*, **9**, 468–472 (in Japanese with English abstract).

Liang, F., and X. A. Xia, 2005: Long-term trends in solar radiation and the associated climatic factors over China for 1961–2000. *Ann. Geophys.*, **23**, 2425–2432.

Pinker, R. T., and I. Laszlo, 1992: Modeling surface solar irradiance for satellite application on a global scale. *J. Appl. Meteorol.*, **31**, 194–211.

Robinson, N., Ed., 1966: *Solar Radiation*. Elsevier, 347pp.

Rossow, W. B., and R. A. Schiffer, 1999: Advances in understanding clouds from ISCCP. *Bull. Amer. Meteor. Soc.*, **80**, 2261–2287.

Trenberth, K. E., J. T. Fasullo, and J. Kiehl, 2009: Earth's global energy budget, *Bull. Amer. Meteor. Soc.*, **90**, DOI:10.1175/2008BAMS2634.1.

Xu, J., 2001: An analysis of the climatic changes in eastern Asia using the potential evaporation. *J. Japanese Soc. Hydro. and Water Resour.*, **14**, 151–170 (in Japanese with English abstract).

Xu, J., and S. Haginoya, 2001: An estimation of heat and water balances in the Tibetan Plateau. *J. Meteor. Soc. Japan*, **79**, 485–504.

Xu, J., S. Haginoya, K. Masuda, and R. Suzuki, 2005a: Heat and water balance estimates over the Tibetan Plateau in 1997–1998. *J. Meteor. Soc. Japan*, **83**, 577–593.

Xu, J., S. Haginoya, K. Saito, and K. Motoya, 2005b: Surface heat and water balance trends in Eastern Asia in the period 1971–2000. *Hydrol. Process.*, **19**, 2161–2186, DOI: 10.1002/hyp.5668.

Xu, J., S. Yu, J. Liu, S. Haginoya, Y. Ishigooka, T.

Kuwagata, M. Hara, and T. Yasunari, 2009: The implication of heat and water balance changes in a lake basin on the Tibetan Plateau, *Hydrolo. Res. Lett.*, **3**, 1–5.

Yang, K., T. Koike, P. Stackhouse, C. Mikovitz, and S. J. Cox, 2006: An assessment of satellite surface radiation products for highlands with Tibet instrument data. *Geophys. Res. Lett.*, **33**, L22403, doi:10.1029/2006GL027640.

Yang, K., R. T. Pinker, Y. Ma, T. Koike, M. Wonsick, S. J. Cox, Y. Zhang, and P. Stackhouse, 2008: Evaluation of satellite estimates of downward shortwave radiation over the Tibetan Plateau. *J. Geophys. Res.*, **113**, D17204, doi:10.1029/2007JD009736.

Yoshida, S., 1970: A method for revising the influence to the sunshine duration rate from topography and buildings. *Tenki*, **17**, 63–68 (in Japanese).